Viscosity of water measurement based on Poiseuille's equation

Jochem Langen
L2 Laboratory Skills, Lab Group H4, Lab partners: Owen Jessop, Manon Jones & Jodie Kelly
Submitted: 11-12-2020; Dates of Experiment: week 45-47

This paper provides a method and experimental results of a water viscosity measurement, using Poiseuille's Equation and Reynolds numbers. From 3 different set ups using bottle containers and capillary tubes, values were obtained of 1.33 ± 0.04, 10.1 ± 0.2 & 3.569 ± 0.013 $mPa\,s$, all in disagreement with literature. Though giving too large errors for good individual fits, systematic errors expected due to the circular tube approximation cause inconsistency and a poor combined fit.

I Introduction

The Poiseuille law, one of the main fluid dynamics equations, was experimentally derived by J. L. M Poiseuille and published in 1840. It described the fluid flow in tubes and came in the form:[1]

$$Q = \frac{K" Pa^4}{L}, \tag{1}$$

where Q is the flow rate, $K"$ a function of temperature (T) and the type of liquid, P the pressure drop across the tube, a the tube radius and L the tube length. This relation was later derived from the Navier-Stokes equations by E. Hagenbach in 1860; for a system where the pressure gradient is caused by a height difference this becomes [1]

$$Q = \frac{\pi \rho g h a^4}{8\eta L}, \tag{2}$$

with ρ the water density, g the gravitational acceleration, h the water height and η the dynamic viscosity: a measure of fluid flow resistance and property of its composition, T and ρ. These equations are valid for incompressible, Newtonian fluids; the latter meaning its shear stress is linearly depended of its velocity gradient by η [2]. In addition, the equations regard laminar flow, having Reynolds Numbers, $Re < 2100$. These can be determined from [2]

$$Re = \frac{v \rho 2a}{\eta}, \tag{3}$$

with v the linear flow speed, defined as Q/S where S is the tube cross-section.

In this work, a simple experiment is detailed and its results analysed; investigating the viscous forces of fluid flow in a capillary tube out of a large water container using Poiseuille's law. Therefrom, tap water η will be ascertained and therewith eq. 2 verified. This equation needs to be rewritten as to obtain variables fit for measurement. To that end, Q is converted to the rate of change in water height $\frac{dh}{dt}$ via

$$Q = -A\frac{dh}{dt}, \tag{4}$$

with A the container cross-sectional area. The resultant differential solves to give

$$h = h_0 e^{-\frac{\pi \rho g a^4}{8\eta L A} t}, \tag{5}$$

where h_0 is the initial water height in the container and t the time. This can be rewritten for time as

$$\frac{\pi \rho g a^4}{8LA} \times t = t_{gen.} = \eta \times ln(h) - \eta \times ln(h_0), \tag{6}$$

where $t_{gen.}$ is a set up generalised time coordinate.

II Methods

The time was measured between set Δh of the water level in the container. $t_{gen.}$ can therewith be obtained from the set up parameters, a, L & A. A is ascertained from the container circumference, C obtained by looping string around it; the string as well as L being measured with a ruler. Alternatively, a was determined by analysing a picture of the tube cross-section in ImageJ to pixel precision, using a ruler as scale. These parameters are marked in Fig. 1.

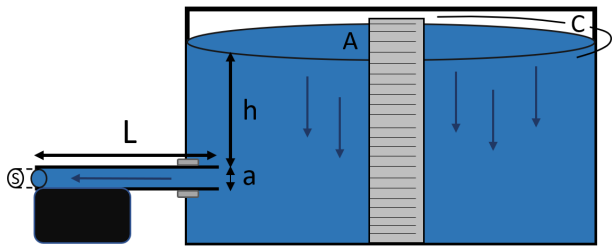

Figure 1: A schematic overview of the set up with the water flowing from the container on the right out of the capillary tube on the left. A ruler is attached to the side of the container.

The receding water level in the container was filmed, the footage of which analysed in frame precision video players like MPC-HC and Aegisub and the timestamps measured. For the container, bottles with as uniform cross-sections as possible were used, mainly being pop bottles; this provides the largest height range for measurements. The capillary tube is inserted in the bottle and sealed using materials like cling film or blu-tack. A support is used to ensure the lack of a vertical component between tube ends. Care is taken to remove air bubbles from the tube before measurements are made. Three set ups were used each producing one data set named Orange, Green & Blue. Orange and Green each consisted of 3 subsets. Only for Orange, repeated T measurements were made of the fluid using a simple thermometer.

III Results

The subsets were combined to get three data sets with average time values for a certain h. Re was calculated for each data point using $\eta_{lit.}$ and eq.3 & 4 with $\frac{dh}{dt}$ approximated as $\frac{\Delta h}{\Delta t}$ between subsequent data points. Non-laminar flow points were discarded. As to merge the data to fit over all the sets and therewith reduce the effect of any unaccounted for parameters or phenomena differing per set up, $t_{gen.}$ is used Orange and Green data sets were scaled up to h_0 of the Blue data set allowing for the data to be merged. The best fit parameters on the data were computed through minimisation of the Chi-squared value of the data performed using the BFGS method with the scipy.optimize Python module. Scaling factors were employed to counter precision losses. The data points, their individual fitted lines and their combined fit are plotted in Fig. 2.

The obtained η values and the corresponding statistical variables can be found in Table 1. For the Orange, Green and Blue data respectively, 100.00%, 88.24% & 100.00% of the Y-residuals and 87.5%, 100.00% & 84.85% of the X-residuals fit in the 1 σ interval containing 68.27% of the

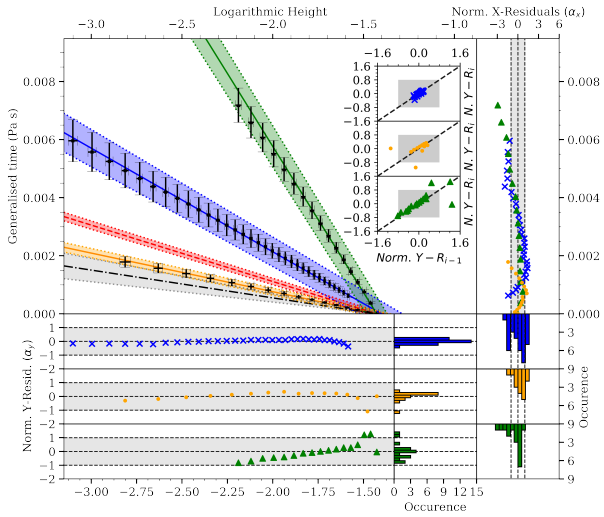

Figure 2: The parameter generalised t against the natural logarithm of h. Each of the three colour-coded data sets include linear χ^2 fitted lines with filled intervals depicting their errors. The red "–" line represents the fit over all data and the black "-." line shows the model according to the $\eta_{lit.}$ (see Table 1, combined), both with error intervals. Normalised Y and X residuals are plotted for each set and lag plots of the normalised Y residuals lagged by 1 are drawn on the top right. An area of 1 and 0.8 standard deviations is filled in for the residual and lag plots respectively.

data in a Gaussian distribution. Particularly for the Green data set a linear relation in the lag plots and corresponding shape in the Y residual plots in Fig. 2 can be observed, indicating a slight error in the fitted model. Similarly, correlated X residual shapes can be observed in the plot.

Data set:	Combined	Orange	Green	Blue
Viscosity, η $(mPa\,s)$	1.94 ± 0.03	1.33 ± 0.04	10.1 ± 0.2	3.569 ± 0.013
χ^2_ν	4e1	1.31e−1	4e−1	2e−1
Cumulative prob., P	0.0	1.0	1.0	1.0
Durbin-Watson statistic, $\mathcal{D}$	X	1.4	0.5	0.2
Temperature, $T\,(K)$	293 ± 10	302.6 ± 0.6	293 ± 10	293 ± 10
Density [3], ρ $(kg\,m^3)$	998 ± 2	995.9 ± 0.8	998 ± 2	998 ± 2
Literature viscosity [4], $\eta_{lit.}$ $(mPa\,s)$	1.0 ± 0.3	0.8101 ± 0.0010	1.0 ± 0.3	1.0 ± 0.3

Table 1: The Viscosity values and statistical results of each data set named according to the colour as in Figure 1; Blue belongs to the top, x; Orange the middle, •; Green the bottom △-marked residuals. No non-zero digits could be extracted from the combined data P value.

IV Discussion

For the individual data sets, the χ^2_ν and P values, being much lower than 1 and very close to 1 respectively indicate a poor fit and suggest overestimated uncertainties. As $\mathcal{D} << 2$, this suggest systematically correlated residuals. Since the η per data set differ far more than σ they can be considered inconsistent with each other. This provides incredibility to the merit of the combined result, which is confirmed by the high χ^2_ν and low P value of the combined fit, suggesting it to be poor and to be questioned. The large uncertainties in T contribute towards this data inconsistency and fluctuations/thermalisation will have altered η during the experiment.

Approximating the gradient to be linear between 2 points as to get the gradient provides an uncertainty in the Reynolds numbers and hence the selection of data used; using eq. 2 or eq. 4 & 5 instead was considered and gives considerably higher numbers using $\eta_{lit.}$. However, as these equations would break down for non-laminar flow this method was abandoned. As all the data is in disagreement with the accepted values, systematic errors/unaccounted effects will been present. These include the viscous forces in the container, though smaller due to the smaller v [2] they will increase the apparent η. The slight Δh between capillary tube ends will still have been present, either increasing or decreasing Q. The non-ideal circular S, having dents and elliptical shapes along its length, means an elliptical Hydraulic radius, R_H should have been used [2]

$$R_H = 2 \times \frac{S}{\mathcal{P}}, \tag{7}$$

with $\mathcal{P}$ the wetted perimeter. Additionally, though care was taken to let them escape before measuring, air bubbles have still briefly been observed at some points along the measurements, decreasing Q through the tube. Leaking has also been detected, though only slight, this will have increased Q so decreased the η estimation. These factors could explain the linear shift of the fitted lines.

Despite the pixel precision the dominant error is still on a due to the 4^{th} power and large SE. Using elliptical analysis would reduce this and potentially splitting the tube up in several sections as well as taking more sets solely changing a will improve its accuracy and the quantify its effect.

V Conclusions

In conclusion, the experimental data follows Poiseuille's relation given the small residuals centred around the mean and the good visual fit, however the χ^2_ν and P values suggest over- & underestimated errors for the individual and combined fits respectively. The former likely due to ellipticity of the tube, supported by the $\mathcal{D}$ statistic suggesting unaccounted correlation. The sets deviate too much for a confident combined result and the Orange, Green & Blue values differ from literature by 64.20%, 950.89% & 272.63% respectively.

References

[1] S. P. Sutera and R. Shalak, The History of Poiseuille's Law, Annual Review Fluid Mech. 1993. 25: 1-19.

[2] F. M. White, Fluid Dynamics, 8^{th} ed., McGraw-Hill US Higher Ed USE Legacy, New York (2015), Ch. 1.7, 6.4, 6.8.

[3] M. Tanaka, G. Girard, R. Davis, A. Peuto and N. Bignell, Recommended table for the density of water between 0 °C and 40 °C based on recent experimental reports, Metrologia 38 301 (2001).

[4] K. Orlov and V. Ochklov, Viscosity of Ordinary Water Substance Calculation based on equations for general and scientific use, MPEI and RNE of IAPWS, last updated: 21/09/2012, URL: http://twt.mpei.ac.ru/mcs/worksheets/iapws/wspsDVRT.xmcd. Accessed on 08/12/2020.

[5] I. G. Hughes, T. P. A. Hase, Measurements and their Uncertainties, A practical guide to modern error analysis, Oxford university press, New York, United States (2010), p. nulla, Ch. 1.3, 2.7, 4.5, 5.3, 6.7, 8.4.

VI Error Appendix

All propagation through Standard Errors or Calculus and Functional methods as well as measurement errors are determined in accordance with Hughes & Hase [5]. Standard Deviations are calculated through the STDEV.S Excel function.

For ρ and $\eta_{lit.}$ the errors were determined as half the calculated value interval given by the uncertainty interval on T and ρ for the latter. The T uncertainty was chosen to be $\pm 10\,K$ due to the difference between cold tap water and room temperature. The consequent intervals are: $995.6 < \rho < 999.7\,kg\,m^{-3}$ [3] & $799.8 < \eta_{lit.} < 1311.6\,\mu Pa\,s$ [4]. In contrast, as T was recorded for the Orange data set with a SE of 0.06 K, an error could be adopted of $0.83\,kg\,m^{-3}$ for ρ, limited by the source [3] and an interval of $809.14 < \eta_{lit.} < 811.10\,\mu Pa\,s$ [4].

The dominant error, coming from a, was determined to be half the error on the diameter, d. This error on d has been taken as the SE of 5 d measurements of a single cross section limited to not be smaller than the length corresponding to one pixel, as the sub-pixel interpolation accuracy could not be safely assumed. These errors on d were combined with the error on the pixel-distance conversion factor according to the Calculus method. The more circular shape of the tube was the main reason for the much smaller error on the Orange set.

Both the errors on L and h were calculated as the difference between measurements of both tube ends or height of the tube and the water respectively. The corresponding errors were determined according to the Calculus method combination of $\sqrt{2}\times$ half the smallest division [5].

The error on C was determined identically, with the addition of a weighted mean error, $\alpha_{\bar{x}}$ out of 3 measurements for the Green data set, following: [5]

$$\alpha_{\bar{x}} = \frac{1}{\sqrt{\sum_j \frac{1}{\alpha_j^2}}}, \tag{8}$$

for the j^{th} measurement. As the video measurement programmes used allowed for frame accuracy measurements, an error on t was adopted of 1/30 s, from the 30 fps video frame-rate. For the Blue data, the Calculus method was utilised for the error propagation for the difference between the measurement and the t offset. There was no starting time offset for the other data. Considering the Orange and Green data sets, the three subsets of t measurements for given h made for a weighted mean combined error as per eq. 8. As the difference between subsets increases for greater t in a seemingly exponential manner, the flexible SE will have been a better representation of the error rather than the weighted mean error. However, as no subsets were available for the Blue data, this could not be done for that set and error extrapolation from visible patterns in the Orange and Green errors did not provide anything worthwhile. Hence, to enhance consistency between data sets, the application of the weighted mean method was kept.

In order to obtain A, the container radius R was required, which was inferred from the circumference C. The error was propagated through the Calculus Method with the following equations:

$$R = C/(2\pi) \tag{9}$$

and

$$A = \pi R^2, \tag{10}$$

with all variables as defined previously. From these variables the error on $t_{gen.}$ was propagated through the Functional method as zero data points are included which are not compatible with the Calculus method (division by 0). This was thus applied to the following equation: [2]

$$t_{gen.} = \frac{\pi \rho g a^4}{8LA} \times t, \tag{11}$$

with all variables defined as aforestated.

The height levels at which the time measurements were made were scaled to the same baseline as the Blue data

$$h_{scaled} = \frac{h}{h_0} \times h_{0,Blue}, \tag{12}$$

after which they were converted to the (natural) logarithmic height bringing it to

$$ln(h_{scaled}) = ln(h) - ln(h_0) + ln(h_{0,Blue}), \tag{13}$$

hence turning the scaling into a simple translation. The consequent errors were calculated using the Calculus method.

The χ^2 minimisation was calculated using the $t_{gen.}$ residuals. The BFGS optimisation algorithm used produces an Hessian matrix, H from which the errors on the parameters are deduced as follows:

$$\alpha_k,\ \alpha_\eta = \sqrt{2 \times diag(H)}, \tag{14}$$

where α_k & α_η are the errors on the intercept, $k = \eta \times ln(h_0)$ and the viscosity, η respectively each corresponding to a diagonal entry of H. To achieve successful optimisation, linear scaling of the variables, errors and estimations had to be performed as to prevent error precision losses. The expectation values, were $\eta_{lit.}$ for η and $\eta_{lit.} \times ln(h_{0,Blue})$ for k conform eq. 6. These were scaled up by a factor of $\mathcal{T} \times \mathcal{H}$ and $\mathcal{T}$ respectively. The $ln(h)$ values were correspondingly scaled down by $\mathcal{H}$ and the $t_{gen.}$ scaled up by $\mathcal{T}$. This gives:

$$t_{gen.}\,\mathcal{T} = (\eta\,\mathcal{T}\,\mathcal{H}) \times (\frac{ln(h)}{\mathcal{H}}) + k\,\mathcal{T}. \tag{15}$$

Consequently, the errors α_k & α_η were both to be be scaled down again by $\mathcal{T}$ and $\mathcal{T} \times \mathcal{H}$ specifically. Ultimately, only $\mathcal{T}$ factors were utilised, ranging in values from 1,000 to 1,000,000. The combined data error was also determined using maxima/minima of the $\chi^2_\nu + 1$ contour plot in $k - \eta$ space, seen in Fig.3; those extrema being at the corresponding $\pm\alpha_{k,\eta}$ interval limits. The α_η found from the plot was $10^2\times$ smaller than from H. To be more pessimistic, the largest of the 2 was chosen to be used. Note also that the plot error does not align with visual observation from Fig. 3. However, this discrepancy does indicate a potential inaccuracy in the algorithm and therewith the fit.

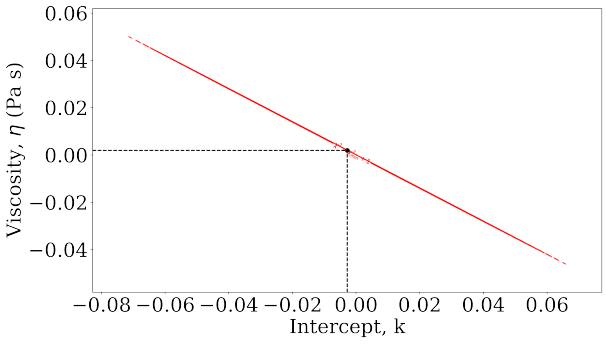

Figure 3: The sharp $\chi^2_\nu + 1$ contour plot of the combined data.